A Study of Age-Related Architectural Changes that Are Most Damaging to Bones

Yan Song,* Michael A. K. Liebschner,† and Gemunu H. Gunaratne*
*Department of Physics, University of Houston, Houston, Texas; and †Department of Bioengineering, Rice University, Houston, Texas

ABSTRACT Osteoporosis-related bone damage causes major socioeconomic problems. For efficient use of therapeutic agents, it is necessary to be able to reliably identify patients with high propensity for nontraumatic fracture. Age-related bone loss imposes several architectural changes in bone; one of the few ways to estimate damage due to individual changes, and hence determine the most serious types of damage, is via the analysis of suitable mathematical models. Anatomical sites such as the vertebral body, proximal femur, and distal radius are locations where most age-related fractures occur. The inner porous (or trabecular) bone from these sites, which resemble disordered cubic networks, play a significant role in load transmission at these sites. Analysis of a mathematical model of porous bone is used to show that perforation of elements of the network is the most damaging architectural change to a bone. We also show that an expression for bone strength, derived on this basis, can capture changes in strength caused by the inclusion of other features like thinning of trabecular bone and the anisotropy of the network. We finally argue that bone density, which is currently the most routinely used diagnostic, cannot be a reliable surrogate for bone strength.

INTRODUCTION

The growth of the older population, and the corresponding increase of osteoporosis and prosthesis, has added to the significance of research into the analysis of mechanical properties of bone. Although there have been recent efforts devoted to addressing this phenomenon (e.g., Kiberstis et al., 2000; Keaveny and Hayes, 1993; Weinstein, 2000; Blank, 2001; Bolotin and Sievänen, 2001), many questions remain to be clarified. One of the more important issues is to determine suitable surrogates for bone strength. The measure most often used for the purpose is bone mineral density, which is routinely estimated using dual energy x-ray absorptiometry (Meunier, 1998). Although higher densities in general correspond to a larger strength and hence a smaller propensity for fracture, there are other factors that play a key role in fracture (McCreadie and Goldstein, 2000; Sandor et al., 1999; Allolio, 1999). In particular, there can be significant changes in microarchitecture that are not captured by bone mineral density.

Large bones from most anatomical sites contain an outer solid segment (known as the cortex) and an inner porous region (referred to as the *trabecular architecture*). Aging causes the cortical bone to become brittle (Mosekilde et al., 1987; Keaveny and Yeh, 2002), and leads to an increasing role for the trabecular bone in transmitting loads (Kiberstis et al., 2000; Keaveny and Hayes, 1993). Trabecular bone is an extremely heterogeneous cellular solid (Keaveny and Yeh, 2002; Gibson and Ashby, 1997), and aging causes changes in factors such as connectivity, trabecular thickness, levels of anisotropy of the network, and changes in material properties. Images of synthetic prototypes of healthy and weak bone samples, shown in Fig. 1, exhibit these architectural changes.

The effective diagnosis and treatment require a comprehensive knowledge of changes that affect bone strength; current experimental techniques are far too rudimentary to achieve this goal. The alternative is to use a suitable mathematical model to first identify the most damaging changes, and use this knowledge to predict changes in bone strength. Confidence in the models can be enhanced by experimental confirmation of these predictions.

Experiments on ex vivo bone samples show that the mean breaking stress $\sigma_{\max}$ of large groups of bone samples reduces with their density ρ, and a power-law relationship (Bell et al., 1967; Carter and Hayes, 1977; McBroom et al., 1985; McElhaney et al., 1970; Rice et al., 1988), as seen here,

$$\sigma_{\max} \sim \rho^{\beta}, \tag{1}$$

has been proposed. The index β varies from $\sim$1.7 in vertebral trabecular bone (Ebbesen et al., 1999) to 2.6 in iliac crest trabecular bone (Ebbesen et al., 1997). This simple empirical description has a straightforward interpretation from uniform isotropic thinning of rod-like and plate-like trabecular bone (Gibson, 1985), but as argued below it is unable to represent variations in breaking stress due to age-related anisotropy or trabecular reduction (for example, the changes of mean thickness of trabecular elements along the axial direction are quite different from those along the off-axial direction). In particular, our results below show that reduction in the number of trabecular elements is most damaging to bone, and hence it is necessary to study a relationship that is based on this mechanism of bone loss.

Submitted May 27, 2004, and accepted for publication August 9, 2004.
Address reprint requests to Yan Song, E-mail: ysong4@mail.uh.edu.

0006-3495/04/12/3642/06 $2.00
doi: 10.1529/biophysj.104.044511

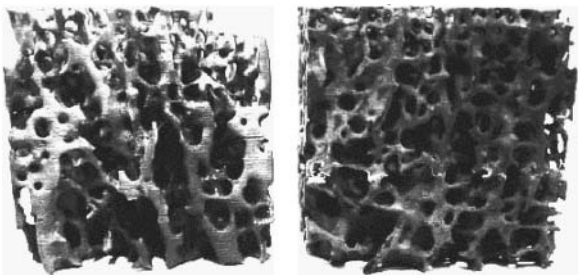

FIGURE 1 Images of synthetic prototypes of a healthy bone (*right*) and a weak bone (*left*). The explicit vertical and horizontal axes of the struts suggest the use of a disordered cubic network model. Note that aging has caused the perforation of the bone and increased the anisotropy of the sample.

Network models of trabecular bone have been analyzed in many studies (Reeve, 1986; Tayyar et al., 1999; Keaveny and Hayes, 1993). A recently proposed Voronoi model (Silva et al., 1995; Silva and Gibson, 1997a,b; Vajjhala et al., 2000; Guo and Kim, 2002; Gibson and Ashby, 1997) has been introduced to study variations in bone strength. In this model, the randomly distributed nodes are connected (if their distance is larger than a predetermined value) to form a network, whose struts are constructed using the Voronoi algorithm (Silva et al., 1995). Results from computational studies indicate that trabecular removal has a more significant effect on strength than trabecular thinning or anisotropy (Guo and Kim, 2002; Vajjhala et al. 2000). According to percolation theory (Stauffer, 1985), if cell elements are randomly removed, the Voronoi network will become more porous and fragile until it is completely separated into many isolated segments when half of the cells are removed; i.e., a Voronoi network has a percolation threshold $\nu_0 = 0.5$. Thus, the fracture load σ_{max} will vanish for nonzero bone density; hence, Eq. 1 cannot represent the relationship between density and strength.

DESCRIPTION OF THE MODEL SYSTEM

In this article, we report conclusions based on a model of trabecular bone that is composed of a disordered cubic network. Locations of nodes of the network are obtained by displacing vertices of a rectangular network of size N_x, N_y, N_z, and sides of length L_x, L_y, and L_z by up to Δ randomly. Struts joining the nearest-neighbor nodes are assumed to be elastic, and their elastic moduli are chosen randomly from a predetermined range $[k_1, k_2]$. Their random values are meant to represent spatial variations in thickness of trabecular elements seen in Fig. 1. Finally, to prevent an entire layer passing through another under compression of the network (glide instability), a bond-bending energy is introduced to change the angles θ between adjacent struts. The corresponding linear coefficients κ are chosen randomly within a predetermined range $[\kappa_1, \kappa_2]$ (Gunaratne et al., 2002). Under an external compression, the system is made to adiabatically approach an equilibrium state that is determined by minimizing the potential energy as

$$U = \frac{1}{2}\sum_{\text{struts}} k(\delta r)^2 + \frac{1}{2}\sum_{\text{bond angles}} \kappa(\delta\theta)^2, \qquad (2)$$

where δr denotes the compression or stretching of a strut and $\delta\theta$ represents the change in a bond angle from equilibrium.

Results reported in this article are obtained for networks with identical properties in the x and y directions. In particular $N_x = N_y$ and $L_x = L_y$. We have also chosen the same ranges $[k_1, k_2]$ for the spring constants in these off-axial directions. We assume that the nodes on the surface of the network cannot move away from it to model the fact that nodes at the cortex do not move inward or outward. The external strain displaces nodes on the top surface by ϵ in the z direction but do not move nodes on the bottom surface in the z direction. All the other nodes on the network are allowed to move freely.

Experiments on the fracture load of trabecular bone from specific anatomical sites have shown that they fail at nearly a fixed level of strain, independent of the age of the subject (Ciarelli et al., 2000; Hogan et al., 2000; Keaveny et al., 1994). It is worth noting that the corresponding fractures stresses can differ by nearly two orders of magnitude (Ebbesen et al., 1997). These conclusions motivate us to use a strain-based criteria for fracture of struts on the network. Previous studies of failure of thin wires (Harlow and Phoenix, 1981) suggest the use of a Weibull distribution, with a cumulative density of $p(\gamma; \eta, \gamma_e) = 1 - e^{-(\gamma/\gamma_e)^\eta}$ to assign the fracture strain γ of struts. Here, the integer η determines the width of distribution; larger values of η correspond to sharper distributions. The mean value of the fracture strains is proportional to γ_e. A second Weibull distribution $P(\gamma;\eta,\gamma_b)$ is used to set the failure of bonds. We study the behavior of the network under adiabatically imposed uniform external strains. Whenever a strut fails, it will be removed along with all associated bond-bending terms in potential energy and it will never be reinstated. The consequence of bond failure is to remove the side that has the weaker coupling constant. We use different random seeds to generate multiple, nominally identical networks.

Fig. 2 shows an example of stress versus strain under compression of such a network. The stress increases nearly linearly with strain until the yield point where the first strut experiences fracture. The stress typically continues to increase until a critical number of struts have failed; the entire network collapses soon after. The maximum value σ_{max} of the stress is considered to be the fracture load of the network. We study how σ_{max} changes when the network is degraded by different mechanisms.

TYPES OF DAMAGE

The aim of our study is to determine the relationship between the density and fracture load of a network when individual

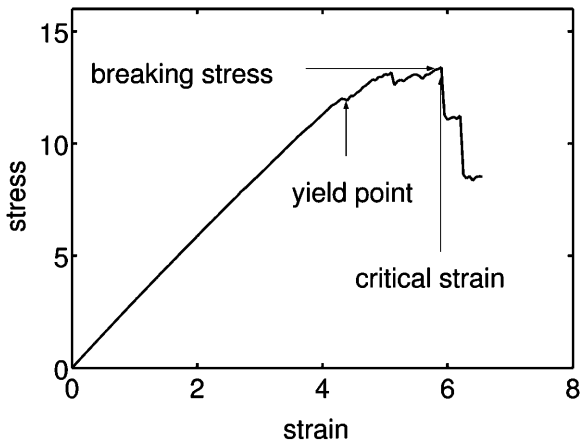

FIGURE 2 Example of stress and strain relation under uniform compression. To compare damage from distinct architectural changes, we relate the reduction in fracture load to the corresponding loss of bone mass.

modes of bone removal are considered separately. In all our analyses, we assume that material properties of bone tissue remain unchanged.

Isotropic thinning of trabecular elements

Let us first consider consequences of isotropic trabecular thinning. Suppose the strength (fracture stress) of the original, complete network is $\sigma_{max}(0)$ and its mass is $m(0)$. Now consider a second network constructed by reducing the cross-sectional area of all struts by a fraction t; thus, the mass of the network is reduced by a fraction t (the length of the rods are constant during thinning) and we assume that the bond-bending coefficient is reduced by t^2. The thinning is implemented in a series of steps; typically t (initially set to 1) is reduced by 0.03 for 25 steps. The breaking stress and mass of each of these 25 networks are calculated as described. Because both the elastic modulus and the mass of each strut depends linearly on its cross-sectional area, σ_{max} and the mass should maintain a linear relationship. Hence, assuming that the contribution to fracture load from the bond-bending terms is not significant, the reduction in fracture load $\sigma_{max}/\sigma_{max}(0)$ will be proportional to the reduction $m/m(0)$ of the mass of the network.

Anisotropic thinning of trabecular elements

There are several distinct ways for a network to be made anisotropic. The mean length of axial trabecular elements can be different from that of off-axial elements. Alternatively, struts along axial and off-axial directions can degrade at different rates. We introduce the following notations to study effects of such changes:

1. Horizontal and vertical struts are thinned by amounts t_H and t_V at each step.
2. The mean length of struts in vertical and horizontal directions are L_V and L_H.
3. Elastic moduli in vertical and horizontal struts, k_V and k_H, span different ranges.

The mass of the system is reduced by the combination of these different factors; for example, in considering anisotropic thinning, reduction in mass will be estimated by using $(S_V L_V/3 + 2S_H L_H/3)$. Here S_V is the cross-sectional area in vertical elements and S_H is that in horizontal elements. After n levels of thinning, cross-sectional areas of vertical and horizontal struts are $S_V = S_{V0}(1–t_V n)$ and $S_H = S_{H0}(1–t_H n)$, where S_{H0} and S_{V0} are the original values of the variables. The corresponding change in mass of the network is

$$m(0) - m(n) \sim n(t_V S_{V0} L_V/3 + 2t_H S_{H0} L_H/3). \quad (3)$$

In this derivation we have noted that one-third of the struts lie along the axial direction, and the remainder in the off-axial directions.

The equivalent spring constant in the anisotropic media is $\sim K = k_V + k_H(\delta z/L_H)$ (the approximation to first term of horizontal contribution as $(\delta x/L_H)^2$), where δz is the deviation of the springs in vertical direction. The breaking stress is thus

$$\tau(0) - \tau(n) \sim (k_V \delta_V + k_H \delta_H \Delta^2/L_H^2)n, \quad (4)$$

where the model parameter $\Delta = \langle \delta z^2 \rangle$. Solving Eq. 3 for n and inserting it into Eq. 4 gives

$$\tau \sim 3\frac{(k_V t_V + k_H t_H(\Delta/L_H)^2)}{2S_H L_H t_H + S_V L_V t_V} m + \text{nonlinear terms}. \quad (5)$$

Thus, the slope of the τ versus m curve will depend on the levels of anisotropy. Nonlinear corrections to the expression can also be relevant.

Random removal of struts

We next consider consequences of random removal of struts from a network. In this scenario, all remaining elements are assumed to retain their strength. Suppose the fraction of elements removed is represented by ν, then the reduction of mass is

$$\frac{m}{m(0)} = 1 - \nu. \quad (6)$$

Previous analysis (Espinoza et al., 2002) on model networks have shown that the reduction in fracture load due to trabecular removal is given by

$$\frac{\sigma_{max}(\nu)}{\sigma_{max}(0)} = \frac{1}{1 + a_1 u^{\psi/2} + a_2 u^{\psi}}, \quad (7)$$

where $\sigma_{max}(\nu)$ denotes the maximum stress of a network with a fraction ν of struts removed, and $\sigma_{max}(0)$ is that of the original unchanged network. The values a_1, a_2, and ψ are parameters that depend on the model. Here

$$u = \frac{logN}{log(\nu_0/\nu)}, \tag{8}$$

where N is the total number of nodes in the network, and $\nu_0 = 0.75$ is the bond percolation threshold (Stauffer, 1985) for cubic networks. When ν approaches ν_0, u becomes large, and Eq. 7 approaches the power-law $\sigma_{max} \sim (\nu_0 - \nu)^{\psi}$.

Damage due to combination of architectural changes

We have studied reductions in fracture load due to a combination of architectural changes. Previous analyses on electrical networks (Espinoza et al., 2002) show that the expression in Eq. 7 can accurately capture the reductions in strength. We will test the validity of this conclusion in our networks.

We use combinations of types of degradation described earlier, and reductions in mass are estimated accordingly. For example, if we are dealing with anisotropic removal of trabecular elements, the mass will be proportional to $(S_V L_V \nu_V/3 + 2S_H L_H \nu_H/3)$. Here ν_H and ν_V are the fractions of horizontal and vertical trabecular removed. We also assume that thinning and trabecular removal are independent processes; thus their combined effect will reduce bone mass according to $(S_V L_V \nu_V t_V/3 + 2S_H L_H \nu_H t_H/3)$.

RESULTS

Trabecular thinning

The results reported below are obtained by computations on five nominally identical model networks. They each have identical control parameters, but are generated using distinct random seeds. The mean and standard deviations of the variables are provided in Table 1.

The star symbols in Fig. 3 represent reduction in fracture load due to isotropic thinning of struts. As expected, the fractional reduction of strength $\sigma_{max}/\sigma_{max}(0)$ bears a linear relationship to the reduction $m/m(0)$ of mass.

The solid circles represent damage due to anisotropic thinning that is predominantly in the axial direction. At each successive stage the thickness t_H of off-axial struts are reduced by 0.017 and that of the axial struts t_V are decreased by 0.030. The plus-sign symbols denote results for networks whose axial and off-axial struts are thinned by 0.017 and 0.030 at each stage. Reductions in mass in these networks are calculated using Eq. 3. Nonlinear corrections to Eq. 5 are apparent in these curves.

TABLE 1 Model parameters on thinning-related processes

	Model parameters
Isotropic thinning	$\gamma_e = 0.1$, $\gamma_b = 0.2$, $\eta = 20$ $L_V = L_H = 10$ $k_V = k_H = 1.0 \pm 0.5$ $\kappa_V = \kappa_H = 5.0 \pm 2.0$ $t_V = t_H = 0.03$
Anisotropic thinning I	$\gamma_e = 0.1$, $\gamma_b = 0.2$, $\eta = 20$ $L_V = 15$, $L_H = 10$ $k_V = k_H = 1.0 \pm 0.5$ $\kappa_V = \kappa_H = 5.0 \pm 2.0$ $t_V = 0.017$, $t_H = 0.030$
Anisotropic thinning II	$\gamma_e = 0.1$, $\gamma_b = 0.2$, $\eta = 20$ $L_V = 15$, $L_H = 10$ $k_V = k_H = 1.0 \pm 0.5$ $\kappa_V = \kappa_H = 5.0 \pm 2.0$ $t_V = 0.030$, $t_H = 0.017$

Trabecular removal

The open circles in Fig. 3 represents reductions in strength caused by random removal at trabecular elements. It is clear that damage caused by removal is far more significant than those due to other factors. As an example, a 30% reduction in mass corresponds to 1), a 30% reduction in fracture load with isotropic thinning; 2), 25% and 40% reductions in fraction loads for the two cases of anisotropic thinning described; and 3) a 70% reduction in fracture load with trabecular removal.

The results from the analysis are displayed in Fig. 3, and the parameters used are summarized in Table 1.

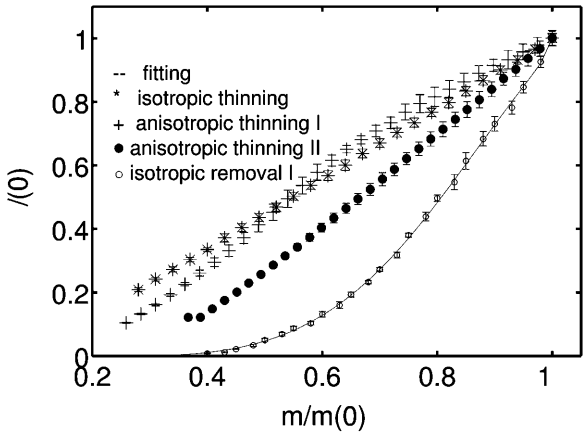

FIGURE 3 Relationships between fracture load and trabecular mass during isotropic (*star symbols*) and anisotropic (*plus signs* and *solid circles*) thinning as well as trabecular removal (*open circles*). The best fit of Eq. 7 for the last case is shown by the dashed line.

Combination of architectural changes

We have studied the damage caused by the implementation of multiple types of architectural changes. Fig. 4 shows results for four such sets described in Table 2. The star and plus in Fig. 4 correspond to isotropic strut removal only, whereas the others include additional types of damage (Table 2). The variations between runs confirm the architecture-dependent behavior of the system, which reinforce previous observations that architecture of the trabecular bones are important in determining the strength (Dempster, 2000; Mosekilde, 2000, 1989). The dashed lines in Fig. 4 represent the best fits of the data to Eq. 7. The parameters a_1, a_2, and ψ are given in Table 2 for each case.

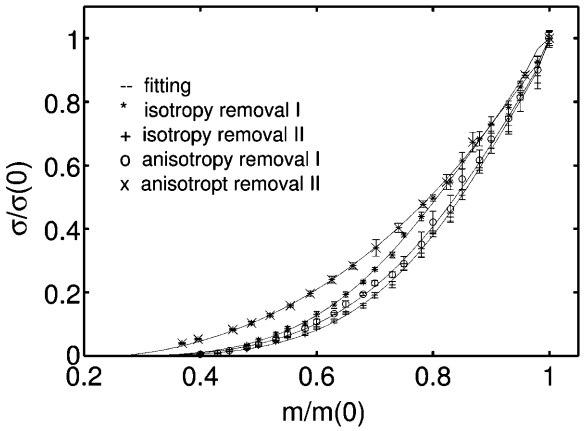

FIGURE 4 Relationship between fracture stress and trabecular mass when isotropic trabecular removal is combined with other architectural changes. The dashed lines in each case represent the best fit to Eq. 7.

CONCLUSIONS

With aging, the solid cortical segments of bone become brittle, and the porous trabecular bone takes a significant role in load transmission. It is thus necessary to be able to reliably estimate the strength of trabecular bone to determine the need for therapeutic intervention. It is difficult to identify such diagnostic tools because the damage to bone arises out of several distinct types of architectural changes. It is thus necessary to first determine the types of age-related architectural changes that are most damaging, and how important the remaining factors are. Use of mathematical models is perhaps the only way to reach this goal.

The analysis of the model system shows that among known age-related architectural changes in bone, trabecular perforation is most damaging. As an example our results show that the loss of strength due to a 30% reduction in mass caused by trabecular removal is more than double the loss due to other architectural changes. This observation suggests that an expression relating the strength and mass of bone based on an expression of trabecular perforation will be able to describe damage due to multiple types of architectural changes. This expectation was validated in the analysis of model networks. However, it is also clear from Fig. 4 that the relationship between fracture load and density of trabecular bone depends on changes in factors such as the level of

TABLE 2 Simulation and fitting parameters at removal-related processes

		Fitting coefficients			
	Description	a_1	α	a_2	χ^2
Isotropic removal I	$\gamma_e = 0.1$, $\gamma_b = 0.2$, $\eta = 20$ $L_V = L_H = 10$ $k_V = k_H = 1.0 \pm 0.5$ $\nu_V = \nu_H = 0.025$ $t_V = t_H = 0$, $\kappa = 5.0 \pm 2.0$	−0.0029 ±0.0118	1.2633 ±0.0824	0.0096 ±0.042	0.6524
Isotropic removal II	$\gamma_e = 0.1$, $\gamma_b = 0.2$, $\eta = 20$ $L_V = L_H = 10$ $k_V = k_H = 1.0 \pm 0.5$ $\nu_V = \nu_H = 0.025$ $t_V = t_H = 0$, $\kappa = 3.0 \pm 1.0$	−0.0049 ±0.0220	1.2870 ±0.1134	0.0144 ±0.0081	1.6671
Anisotropic removal I	$\gamma_e = 0.1$, $\gamma_b = 0.2$, $\eta = 20$ $L_V = L_H = 10$ $k_V = 1.5 \pm 1.0$, $k_H = 1.0 \pm 0.5$ $\nu_V = \nu_H = 0.025$ $t_V = t_H = 0$, $\kappa = 5.0 \pm 2.0$	−0.0208 ±0.020	1.1707 ±0.0783	0.0213 ±0.0083	0.3431
Anisotropic removal II	$\gamma_e = 0.1$, $\gamma_b = 0.2$, $\eta = 20$ $L_V = 15$, $L_H = 10$ $k_V = 1.5 \pm 1.0$, $k_H = 1.0 \pm 0.5$ $\nu_V = 0.015$, $\nu_H = 0.025$ $t_V = 0.017$, $t_H = 0.030$ $\kappa = 5.0 \pm 2.0$ $\kappa = 5.0 \pm 2.0$	−0.1856 ±0.1921	0.7382 ±0.0692	0.1096 ±0.1224	1.8107

trabecular thinning and anisotropy. Consequently, bone density (mass per unit volume) cannot be expected to be a reliable surrogate for the fracture load of a bone.

The authors thank J. Espinoza-Ortiz and C. Rajapaske for discussion.

This research was partially funded by a grant from the National Science Foundation (Y.S., G.H.G.).

REFERENCES

Allolio, B. 1999. Risk factors for hip fracture not related to bone mass and their therapeutic implications. *Osteoporos. Int.* S2:S9–S16.

Bell, G. H., O. Dunbar, J. S. Beck, and A. Gibb. 1967. Variations in strength of vertebrae with age and their relation to osteoporosis. *Calcif. Tissue Res.* 1:75–86.

Blank, R. D. 2001. Breaking down bone strength: a perspective of the future of skeletal genetics. *J. Bone Min. Res.* 16:1207–1211.

Bolotin, H. H., and H. Sievänen. 2001. Inaccuracies inherent in dual-energy x-ray absorptiometry in vivo bone mineral density can seriously mislead diagnostic/prognostic interpretation of patient-specific bone fragility. *J. Bone Min. Res.* 16:799–805.

Carter, D. R., and W. C. Hayes. 1977. The compressive behavior of bone as a two-phase porous structure. *J. Bone Min. Res.* 15:32–40.

Ciarelli, T. E., D. P. Fyhrie, M. B. Schaffler, and S. A. Goldstein. 2000. Variations in three-dimensional cancellous bone architecture of proximal femur in female hip fractures and in controls. *J. Bone Min. Res.* 15: 32–40.

Dempster, D. W. 2000. The contribution of trabecular architecture to cancellous bone quality. *J. Bone Min. Res.* 15:20–23.

Ebbesen, E. N., J. S. Thomsen, H. Beck-Nielsen, H. J. Nepper-Rasmussen, and L. Mosekilde. 1999. Lumbar vertebral body compressive strength evaluated by dual-energy x-ray absorptiometry, quantitative computed tomography and ashing. *Bone.* 25:713–724.

Ebbesen, E. N., J. S. Thomsen, and L. Mosekilde. 1997. Nondestructive determination of iliac crest cancellous bone strength by pQCT. *Bone.* 21:535–540.

Espinoza, O. J. S., C. S. Rajapaske, and G. H. Gunaratne. 2002. Strength reduction in electrical and elastic networks. *Phys. Rev. B.* 66:144203-1–144203-8.

Gibson, L. J. 1985. The mechanical behavior of cancellous bone. *J. Biomech.* 18:317–328.

Gibson, L. J., and M. F. Ashby. 1997. Cellular Solids: Structure and Properties. Cambridge University Press, Cambridge, UK.

Gunaratne, G. H., C. S. Rajapakse, K. E. Bassler, K. K. Mohanty, and S. J. Wimalawansa. 2002. A model for bone strength and osteoporotic fracture. *Phys. Rev. Lett.* 88:068101-1–068101-4.

Guo, X. E., and C. H. Kim. 2002. Mechanical consequences of trabecular bone loss and its treatment: a three-dimensional model simulation. *Bone.* 30:404–411.

Harlow, D. G., and S. L. Phoenix. 1981. Probability distributions for the strength of composite-materials. II. A convergent sequence of tight bounds. *Intl. J. Fracture.* 17:601–630.

Hogan, H. A., S. P. Ruhmann, and H. W. Sampson. 2000. The mechanical properties of cancellous bone in the proximal tibia of ovariectomized rats. *J. Bone Min. Res.* 15:284–292.

Keaveny, T., and W. C. Hayes. 1993. A 20-year perspective on the mechanical properties of trabecular bone. *Trans. ASME.* 115:534–542.

Keaveny, T. M., and O. C. Yeh. 2002. Architecture and trabecular bone—toward an improved understanding of the biomechanical effects of age, sex and osteoporosis. *J. Musculoskel. Neuron Interact.* 2:205–208.

Keaveny, T. M., E. F. Wachtel, C. M. Ford, and W. C. Hayes. 1994. Differences between the tensile and compressive strengths of bovine tibial trabecular bone depend on modulus. *J. Biomech.* 27:1137–1146.

Kiberstis, P., O. Smith, and C. Norman. 2000. Bone health in the balance. *Science.* 289:1497.

McBroom, R. J., W. C. Hayes, W. T. Edwards, R. P. Goldberg, and A. A. White, Iii. 1985. Prediction of vertebral body compressive fracture using quantitative computed tomography. *J. Bone Joint Surg. Am.* 67:1206–1214.

McCreadie, B. R., and S. A. Goldstein. 2000. Biomechanics of fracture: is bone mineral density sufficient to assess risk? *J. Bone Min. Res.* 15: 2305–2308.

McElhaney, J. H., J. L. Fogle, J. W. Melvin, R. R. Haynes, V. L. Roberts, and N. M. Alem. 1970. Mechanical properties of cranial bone. *J. Biomech.* 3:495–511.

Meunier, P. J. 1998. Osteoporosis: Diagnosis and Management. Martin-Dunitz, London, UK.

Mosekilde, L. 1989. Sex differences in age-related loss of vertebral trabecular bone mass and structure—biomechanical consequences. *Bone.* 10:425–432.

Mosekilde, L. 2000. Age changes in bone mass, structure, and strength—effects of loading. *Z. Rheumatol.* 59:S1–S9.

Mosekilde, L., L. Mosekilde, and C. C. Danielsen. 1987. Biomechanical competence of vertebral trabecular bone in relation to ash density and age in normal individuals. *Bone.* 8:79–85.

Reeve, J. 1986. A stochastic analysis of iliac trabecular bone dynamics. *Clin. Orthop. Rel. Res.* 213:264–278.

Rice, J. C., S. C. Cowin, and J. A. Bowman. 1988. On the dependence of the elasticity and strength of cancellous bone on apparent density. *J. Biomech.* 21:155–168.

Sandor, T., D. Felsenberg, and E. Brown. 1999. Comments on the hypotheses underlying fracture risk assessment in osteoporosis as proposed by the World Health Organization. *Calcif. Tissue Int.* 64: 267–270.

Silva, M. J., W. C. Hayes, and L. J. Gibson. 1995. The effects of nonperiodic microstructure on the elastic properties of two-dimensional cellular solids. *Int. J. Mech. Sci.* 37:1161–1177.

Silva, M. J., and L. J. Gibson. 1997a. Modeling the mechanical behavior of vertebral trabecular bone: effects of age-related changes in microstructure. *Bone.* 21:191–199.

Silva, M. J., and L. J. Gibson. 1997b. The effects of non-periodic microstructure and defects on the compressive strength of two-dimensional cellular solids. *Int. J. Mech. Sci.* 39:549–563.

Stauffer, D. 1985. Introduction to Percolation Theory. Taylor and Francis, London, UK.

Tayyar, S., P. S. Weinhold, R. A. Butler, J. C. Woodard, L. D. Zardiackas, K. R. St. John, J. M. Bledsoe, and J. A. Gilbert. 1999. Computer simulation of trabecular remodeling using a simplified structure model. *Bone.* 25:733–739.

Vajjhala, S., A. M. Kraynik, and L. J. Gibson. 2000. A cellular solid model for modulus reduction due to resorption of trabecular bone. *J. Biomed. Eng.* 122:511–515.

Weinstein, R. S. 2000. True strength. *J. Bone Min. Res.* 15:621–625.